Carbohydrate Polymers 343 (2024) 122493

Contents lists available at ScienceDirect

Carbohydrate Polymers

journal homepage: www.elsevier.com/locate/carbpol

Characterization of cellulases from softening fruit for enzymatic depolymerization of cellulose

Hilary Edema [a,b], Muhammad Furqan Ashraf [a,b], Amos Samkumar [b,c], Laura Jaakola [b,d], Katja Karppinen [a,b,*]

[a] The Arctic Centre for Sustainable Energy, UiT The Arctic University of Norway, Tromsø 9037, Norway
[b] Department of Arctic and Marine Biology, UiT The Arctic University of Norway, Tromsø 9037, Norway
[c] Department of Plant Science, Norwegian University of Life Sciences, Ås 1430, Norway
[d] Division of Food Production and Society, Norwegian Institute of Bioeconomy Research (NIBIO), Ås 1431, Norway

ARTICLE INFO

Keywords:
Cellulose hydrolysis
Cell wall
Endo-β-1,4-glucanase
Glycoside hydrolase family 9 (GH9)
Hemicellulose
Vaccinium myrtillus

ABSTRACT

Cellulose is a major renewable resource for a wide variety of sustainable industrial products. However, for its utilization, finding new efficient enzymes for plant cell wall depolymerization is crucial. In addition to microbial sources, cellulases also exist in plants, however, are less studied. Fleshy fruit ripening includes enzymatic cell wall hydrolysis, leading to tissue softening. Therefore, bilberry (*Vaccinium myrtillus* L.), which produces small fruits that undergo extensive and rapid softening, was selected to explore cellulases of plant origin. We identified 20 glycoside hydrolase family 9 (GH9) cellulases from a recently sequenced bilberry genome, including four of which showed fruit ripening-specific expression and could be associated with fruit softening based on phylogenetic, transcriptomic and gene expression analyses. These four cellulases were secreted enzymes: two B-types and two C-types with a carbohydrate binding module 49. For functional characterization, these four cellulases were expressed in *Pichia pastoris*. All recombinant enzymes demonstrated glucanase activity toward cellulose and hemicellulose substrates. Particularly, VmGH9C1 demonstrated high activity and ability to degrade cellulose, xyloglucan, and glucomannan. In addition, all the enzymes retained activity under wide pH (6–10) and temperature ranges (optimum 70 °C), revealing the potential applications of plant GH9 cellulases in the industrial bioprocessing of lignocellulose.

1. Introduction

Cellulose is the most abundant organic compound and biopolymer on Earth, with an estimated annual production of 15×10^{12} tons of the total biomass produced by photosynthetic organisms (Gupta et al., 2013). As a result, cellulose is an important renewable resource for sustainable production of biofuels and other bio-based chemicals, polymers, composites, and nanomaterials (Costa et al., 2020; He et al., 2023; Li et al., 2021; Seddiqi et al., 2021), without compromising global food security. Cellulose, which is the major structural element in plant cell walls, comprises a large number of glucose units linked through β-(1,4)-glycosidic bonds to form linear chains which are parallelly aligned to enable inter-chain hydrogen bonding, giving rise to a highly organized crystalline structure (Zugenmaier, 2021). The high degree of polymerization and crystallinity provide cellulose with exceptional mechanical strength, which is necessary for its biological roles in plants. Hemicelluloses such as xyloglucan (XG) form tight networks with cellulose microfibrils via hydrogen bonding and act as shields to protect the cellulose skeleton. These attributes combined with further cross-linking with other polymers make plant cell walls resistant to degradation and impede utility of cellulose as a bioresource (Zoghlami & Paës, 2019).

The most sustainable, energy-efficient and non-pollutive option for plant biomass depolymerazation is considered to be the use of specific hydrolytic carbohydrate active enzymes (CAZymes) and proteins (Ejaz et al., 2021; Menon & Rao, 2012; Vasić et al., 2021). Cellulases facilitate hydrolysis of the cellulose and hemicellulose fractions of plant biomass into soluble fermentable sugars. Cellulases remain an important class of industrial enzymes because of their wide range of applications and are expected to play a key role in the transition to industrial-scale lignocellulosic biomass-based 2nd generation biofuel production (Ejaz et al.,

* Corresponding author at: The Arctic Centre for Sustainable Energy, UiT The Arctic University of Norway, Tromsø 9037, Norway.
E-mail addresses: hilary.edema@uit.no (H. Edema), muhammad.f.ashraf@uit.no (M.F. Ashraf), amos.s.premkumar@nmbu.no (A. Samkumar), laura.jaakola@uit.no (L. Jaakola), katja.karppinen@uit.no (K. Karppinen).

https://doi.org/10.1016/j.carbpol.2024.122493
Received 29 February 2024; Received in revised form 11 July 2024; Accepted 12 July 2024
Available online 14 July 2024

2021; Gupta et al., 2013), highlighting the crucial need to investigate cellulases. The filamentous fungi *Trichoderma* spp. is the most widely investigated source of cellulases (Ejaz et al., 2021; Menon & Rao, 2012). However, the enzymatic hydrolysis of lignocellulosic plant material remains a bottleneck for cellulose utilization because of the prohibitive costs and low catalytic efficiencies of the currently used enzymes (Menon & Rao, 2012; Vasić et al., 2021). Therefore, efforts have been made to improve the cost-effectiveness of the hydrolytic process by identifying more efficient and stable enzymes (Maitan-Alfenas et al., 2015). The extensive sequencing of the genomes of diverse organisms in recent years has opened new frontiers for searching new enzymes beyond traditional fungal and bacterial origins, such as wood-feeding insects (Ceja-Navarro et al., 2019; Cragg et al., 2015; Victorica et al., 2020; Willis et al., 2016).

Plants possess the innate ability to efficiently rearrange and degrade their own cell walls via enzymatic cleavage of cell wall polymers and polysaccharides during many developmental processes. Plants, similar to microbes, show a remarkable ability to colonize and thrive in a wide range of environments, from mild to extreme conditions, invade and infect other plants through parasitic interactions, and fight-off pathogenic microbes. These properties represent millions of years of evolution, resulting in cumulative biochemical and physiological adjustments for fitness. However, plants remain poorly screened for cell wall hydrolyzing enzymes, while they could be sources of novel enzymes with the potential to overcome the recalcitrance of lignocellulose biomass (Grandis et al., 2014; Kundu & Sharma, 2018; Lopez-Casado et al., 2008; Tavares et al., 2015).

All known plant cellulases belong to the glycosyl hydrolase family 9 (GH9), which possess a highly conserved GH9 catalytic domain (del Campillo, 1999). Several GH9 members have been identified in different plant species, including *Arabidopsis thaliana* (24), *Hordeum vulgare* (22), *Oryza sativa* (24), *Populus* spp. (25), *Cucumis melo* (melon; 18), *Carica papaya* (papaya; 18), *Litchi chinensis* (litchi; 20), and *Vitis vinifera* (grapevine; 24) (Buchanan et al., 2012; Du et al., 2015; Li et al., 2015; Ming et al., 2008; Zhu et al., 2023). The members of this family are divided into three structural subfamilies (Urbanowicz, Bennett, et al., 2007). In contrast to subfamily A (GH9A) members, which are membrane-bound and required for cellulose biosynthesis (Mølhøj et al., 2002), cellulases of B (GH9B) and C (GH9C) subfamilies consist of secreted *endo*-β-(1,4)-glucanases (EC 3.2.1.4) capable of cellulose degradation in the plant cell wall by cleaving internal β-1,4-linkages. Furthermore, GH9C proteins contain a carbohydrate binding module 49 (CBM49) at the C-terminus for binding crystalline cellulose (Kundu & Sharma, 2018; Urbanowicz, Bennett, et al., 2007), implying that members of this subfamily exhibit high affinity for and the potential to degrade recalcitrant cellulose (Lopez-Casado et al., 2008; Urbanowicz, Catalá, et al., 2007). The members of GH9B and GH9C have been reported to remodel plant cell walls during various developmental processes (Grandis et al., 2019; He et al., 2018; Li et al., 2019; Zhu et al., 2023).

One of the developmental processes in which plants utilize hydrolytic CAZymes is the softening of fleshy fruits during fruit ripening. The irreversible disassembly and hydrolysis of cell wall polysaccharides due to the coordinated action of different CAZymes, especially glycoside hydrolases (GHs), is the major process responsible for fruit softening (Moya-León et al., 2019; Peng et al., 2022; Shi et al., 2023; Su et al., 2024). The decrease in fruit firmness during ripening has been shown to correlate with reductions in the amount of cell wall polysaccharides, including cellulose and hemicelluloses, and an increase in hydrolytic enzyme activities, including total cellulase activity, indicating cell wall depolymerization (Elhassan & Abu-Goukh, 2016; Figueroa et al., 2010; Liu et al., 2021; Zhang et al., 2019). Ripening-specific cellulases have been described in many fruits (Chourasia et al., 2008; Lashbrook et al., 1994; Mejía-Mendoza et al., 2022; Real et al., 2004) and some of their roles in fruit softening and cell wall depolymerization have been verified by gene overexpression or silencing studies (Lee & Kim, 2011; Su et al., 2024; Zhang et al., 2023). Recently, blackberry RuEG6, a fruit ripening-specific C-type *endo*-β-(1,4)-glucanase, was reported to cause increased cellulase activity leading to significant reduction in cellulose content and thinner leaves when overexpressed in tobacco leaves (Zhang et al., 2023). However, the role of cellulases in fruit softening remains largely unclear and may vary between different fruits.

The degree of fruit softening can range from moderate softening and textural changes, such as in apples (*Malus* × *domestica*), to extensive softening of fruit pulp, leading to a juicy texture in tomato (*Solanum lycopersicum*) and berries, such as bilberry (*Vaccinium myrtillus*). We have previously shown that a wide range of CAZyme-encoding genes are activated during bilberry fruit ripening and that these genes are positively regulated by the ripening inducing abscisic acid (ABA) hormone (Karppinen et al., 2018). As bilberry fruits undergo rapid and extensive softening during ripening, leading to juicy flesh and a short shelf-life of berries, we hypothesized that the ripening berries could reveal cellulases with a high potential for depolymerization of cellulose and possibly hemicelluloses.

In the present study, we identified 20 GH9 cellulases from a recently sequenced genome of bilberry (Wu et al., 2022). Based on transcriptome and RT-qPCR analyses, two B-type and two C-type cellulases showed fruit ripening-specific expression patterns. When these cellulases were expressed in *Pichia pastoris,* the recombinant enzymes exhibited hydrolytic activity on various cellulose and hemicellulose substrates. Furthermore, the bilberry cellulases retained enzymatic activity over wide pH and temperature ranges and were thermo-stable at 30 to 70 °C, demonstrating that plants harbor cellulases with biochemical properties beneficial for industrial applications.

2. Materials and methods

2.1. Plant materials

Bilberry (*Vaccinium myrtillus* L.) fruits at different ripening stages, from 3.0 to 5.0 were collected in a previous study (Wu et al., 2022) and stored at −80 °C. Bilberry tissue samples were collected from forest stands in Oulu (65°01′ N, 25°28′ E). ABA [(±)-abscisic acid; Sigma-Aldrich, St. Louis, MO, USA] treatments (0.5 mM ABA, 2 mM ABA, or water as negative control) of bilberry fruits were conducted in Petri dishes under sterile conditions as described earlier (Karppinen et al., 2018) and samples were collected after 48 h from the beginning of the treatment.

2.2. Identification and sequence analysis of cellulase genes in bilberry genome

Protein sequences corresponding to plant GH9 enzymes were downloaded from the Carbohydrate Active Enzymes database (Drula et al., 2022; http://www.cazy.org). The protein sequences were subjected to multiple sequence alignment using MUSCLE (Madeira et al., 2022) and the alignment was used to generate a Hidden Markov Model (HMM) profile of the GH9 protein sequences using HMMER software (version 3.3.2) with default parameters (Potter et al., 2018). The GH9 HMM profile was used to search a database of bilberry proteome downloaded from the Genome Database for Vaccinium (https://www.vaccinium.org). Significant hits with *E*-value $\leq 10^{-6}$ were analyzed using the NCBI Conserved Domains Database (Wang et al., 2023; http://www.ncbi.nlm.nih.gov/Structure/cdd/cdd.shtml) to verify the presence of conserved domains and residues for catalytic activity. Transmembrane domains were predicted using DeepTMHMM v.2.0 (https://dtu.biolib.com/DeepTMHMM) and CCTop (https://cctop.ttk.hu/job/submit). Signal sequences and cleavage sites were predicted using PrediSi (Hiller et al., 2004; http://www.predisi.de/), TargetP-2.0 (Almagro Armenteros et al., 2019; https://services.healthtech.dtu.dk/services/TargetP-2.0/) and SignalP-6.0 (https://services.healthtech.dtu.dk/services/SignalP-6.0/). The physicochemical properties of the

proteins were determined using the ProtParam tool (Duvaud et al., 2021). The accession numbers for all the identified bilberry GH9 sequences are shown in Table 1.

2.3. Phylogenetic analysis

Phylogenetic analysis of GH9 protein sequences was conducted using MEGA software version 11 (Tamura et al., 2021). Multiple sequence alignments were performed using the MUSCLE program in MEGA 11. A phylogenetic tree was constructed using the Maximum Likelihood method with 1000 bootstrap estimates. The accession numbers for all GH9 sequences used in the phylogenetic analysis are listed in **Supplementary Table S1**.

2.4. Gene expression analysis from transcriptome

An earlier transcriptome dataset generated from ripening bilberry fruit was utilized in this study (Samkumar et al., 2021). Raw reads from the RNA-Seq data are stored under the BioProject ID PRJNA747684 in the NCBI-SRA database. The expression of all bilberry cellulase genes was retrieved from the transcriptome data. Briefly, the reads were aligned to the protein-coding genes of the bilberry reference genome obtained from Genome Database for Vaccinium (https://www.vaccinium.org/). The number of reads mapped to every individual GH9 gene provided a raw count using the HTSeq tool (Anders et al., 2015). Count values were used to calculate the normalized expression levels as Fragments Per Kilobase of transcript per Million mapped reads (FPKM) from three biological replicates. In the current study, to obtain the expression values of GH9 genes in terms of FPKM counts, we used only the genes annotated and classified earlier as GH9 cellulases from Kyoto Encyclopedia of Genes and Genomes (KEGG) pathway enrichment analysis of the transcriptome.

2.5. RNA isolation and RT-qPCR analysis

Frozen tissues and fruits samples were homogenized into a fine powder using a mortar and pestle under liquid nitrogen. Total RNA was extracted from approximately 100 mg of tissue powder using the Spectrum™ Plant Total RNA kit (Sigma-Aldrich) with on-column DNase I (Sigma-Aldrich) digestion following the manufacturer's protocol. Quality of RNA was checked and quantified using a NanoDrop spectrophotometer (Thermo Fischer Scientific, Waltham, MA, USA) and integrity was verified by agarose gel electrophoresis. Total RNA (2.5 μg) was converted to cDNA using the SuperScript™ IV First-Strand Synthesis System (Thermo Fisher Scientific), following the manufacturer's instructions. From ABA-treated berries, total RNA was extracted and cDNA synthesized as described previously (Karppinen et al., 2018).

RT-qPCR analysis was performed using a Bio-Rad CFX96™ Real Time System (Bio-Rad, Hercules, CA, USA) and SsoAdvanced™ Universal SYBR Green Supermix (Bio-Rad). The PCR conditions were: 95 °C for 30 s, 40 cycles of 95 °C for 5 s, and 60 °C for 10 s, followed by a melting curve analysis ranging from 65 °C to 95 °C with increments of 0.5 °C per cycle, to validate the amplification of only one product. Gene-specific primer pairs were designed using the Primer3 tool v.0.4.0 (Untergasser et al., 2012; https://bioinfo.ut.ee/primer3-0.4.0/) and the primer sequences used in this study are shown in **Supplementary Table S2**. The RT-qPCR reactions were performed with at least three biological replicates. The normalized expression levels of GH9 genes were calculated using a CFX Maestro™ Software (Bio-Rad) using glyceraldehyde-3-phosphate dehydrogenase (*GAPDH*) and actin (*ACT*) as reference genes.

2.6. Gene cloning

The coding sequences (CDSs) of the four selected cellulase genes were amplified by PCR from bilberry fruit cDNA using Phusion® High-Fidelity DNA Polymerase (Thermo Fischer Scientific) with gene-specific primers that excluded native signal sequences (**Supplementary Table S3**). The amplified CDSs were separately inserted into *Eco*RI/*Sal*I or *Kpn*I/*Sal*I restriction sites in the yeast expression vector pPICZαA, which included a N-terminal α-factor secretion signal and C-terminal hexahistidine (6xHis) tag. The vector constructs were verified by Sanger sequencing using a BigDye™ Terminator Cycle Sequencing Kit (Applied Biosystems, Foster City, CA, USA) and sequencing was performed at the UiT The Arctic University of Norway sequencing facility on a 3130xl Genetic Analyzer (Applied Biosystems).

2.7. Protein expression and Western blot

The constructed expression vectors were separately transformed into electrocompetent *Pichia pastoris* SMD strain by electroporation using GenePulser Xcell™ electroporator (Bio-Rad) followed by selection of

Table 1
Physicochemical properties of bilberry cellulases.

Accession ID	Gene	CDS (bp)	Protein (AA)	Molecular weight (kDa)	p*I*	GRAVY	Protein domains	Subfamily
Vmy09g22948.t1	*VmGH9A1*	1854	617	68.24	8.93	−0.338	TMD, GH9	A
Vmy09g22680.t1	*VmGH9A2*	1881	626	69.94	7.23	−0.356	TMD, GH9	A
Vmy05g11690.t1	*VmGH9A3*	1275	424	46.73	5.23	−0.262	TMD, GH9	A
Vmy07g26194.t1	*VmGH9A4*	1389	462	50.72	4.94	−0.325	SP, GH9	A
Vmy02g32865.t1	*VmGH9B1*	1491	496	54.54	5.18	−0.319	SP, GH9	B
Vmy06g33485.t1	*VmGH9B2*	1431	476	52.55	5.51	−0.292	SP, GH9	B
Vmy10g11297.t1	*VmGH9B3*	1524	507	56.18	5.11	−0.109	SP, GH9	B
Vmy12g2938.t1	*VmGH9B4*	1533	510	56.70	8.81	−0.293	SP, GH9	B
Vmy12g1188.t1	*VmGH9B5*	1497	498	54.39	5.37	−0.278	SP, GH9	B
Vmy10g10315.t1	*VmGH9B6*	1494	497	54.77	6.97	−0.182	SP, GH9	B
Vmy01g16063.t1	*VmGH9B7*	1569	522	58.42	6.08	−0.352	SP, GH9	B
Vmy04g26856.t1	*VmGH9B8*	1572	523	59.03	6.45	−0.471	SP, GH9	B
Vmy02g31074.t1	*VmGH9B9*	1482	493	54.48	7.57	−0.237	SP, GH9	B
Vmy12g1323.t1	*VmGH9B10*	1548	515	56.09	6.45	−0.252	SP, GH9	B
VmyS31436g29709.t1	*VmGH9B11*	1431	476	52.37	7.27	−0.160	SP, GH9	B
Vmy01g17256.t1	*VmGH9B12*	1599	532	58.36	8.28	−0.197	SP, GH9	B
Vmy10g11296.t1	*VmGH9B13*	1494	497	54.68	5.43	−0.017	SP, GH9	B
Vmy04g28274.t1	*VmGH9B14*	1425	474	52.48	8.73	−0.292	SP, TMD, GH9	B
Vmy12g1268.t1	*VmGH9C1*	1890	629	68.85	8.64	−0.310	SP, GH9, CBM	C
Vmy10g9220.t1	*VmGH9C2*	1782	593	64.44	5.20	−0.261	SP, GH9, CBM	C

CDS, coding sequence; bp, base pair; AA, amino acid; kDa, kilodalton; p*I*, isoelectric point; TMD, transmembrane domain; GH9, glycoside hydrolase family 9 catalytic domain; SP, signal peptide; CBM, carbohydrate binding module.

transformants on YPD media with 100 μg ml^{-1} zeocin. *P. pastoris* transformed with an empty vector was used as the negative control. Protein expression was conducted as described in the EasySelect™ *Pichia* Expression Kit (Thermo Fisher Scientific) with slight modifications. Protein expression was induced by adding 2 % methanol every 12 h. After 7 days of induction, the culture medium was centrifuged at 10,000*g* for 10 min at 4 °C and the supernatant containing the recombinant enzyme was collected.

Total proteins (10 μg) were separated on 12 % sodium dodecylsulphate polyacrylamide gel (SDS-PAGE) using a Mini-Protean II® electrophoresis system (Bio-Rad). The proteins were then transferred onto a 0.2 μm polyvinylidene difluoride (PVDF) membrane using the Trans-Blot® SD Semi-Dry Transfer Cell (Bio-Rad). His-tagged recombinant cellulases were detected using the SuperSignal™ West HisProbe Kit (Thermo Fisher Scientific), according to the manufacturer's instructions. The buffer was exchanged to reaction buffers described below using Pierce™ Protein Concentrators PES, 10K MWCO, 0.5–100 mL (Thermo Fisher Scientific), following the manufacturer's protocol. Protein concentrations were measured using the Quick Start™ Bradford Protein Assay kit (Bio-Rad) with bovine serum albumin (BSA) as a standard, following the manufacturer's instructions.

2.8. Cellulase activity assay

To quantify cellulase activity, the amount of reducing sugars/ends released by incubating a known amount of each enzyme with a given substrate was measured using the 3,5-dinitrosalicylic acid (DNS) method (Miller, 1959). The optimal pH for each enzyme was determined using different 50 mM buffer solutions: sodium citrate (pH 3–6), sodium phosphate (pH 7), and Tris-HCl (pH 8–10). Reaction mixture of 200 μL containing 20 μL of crude protein with 1 % carboxymethylcellulose (CMC; Sigma-Aldrich; 217274) was incubated at 40 °C for 30 min at pH ranging 3–10. The reaction products were mixed with 300 μL of DNS reagent, boiled for 15 min, and rapidly cooled to room temperature. The absorbance of each solution was measured at 540 nm using a microplate reader (Epoch; Bio-Tek, Winooski, VT, USA). The effect of temperature was evaluated from 20 to 80 °C at optimal pH. Thermal stability was assessed by pre-incubating each enzyme in a 50 mM buffer at the optimal pH in the presence of 10 % glycerol without a substrate. The enzyme solutions were pre-incubated at different temperatures from 30 to 80 °C for 30, 60, 90, and 120 min. Residual enzyme activity on CMC was subsequently measured as described above and expressed as a percentage of the maximum enzyme activity at 0 min of pre-incubation.

Substrate specificity of the cellulases was evaluated at optimal pH and temperature on 1 % CMC, 1 % microcrystalline cellulose Avicel® PH-101 (Sigma-Aldrich; 11365), 1 % phosphoric acid swollen cellulose (PASC) generated from microcrystalline cellulose Avicel® PH-101 (Zhang et al., 2006), 1 % glucomannan (GM) from konjac (Megazyme, Wicklow, Ireland; P-GLCML, >98 %), 1 % xyloglucan (XG) from tamarind seed (Megazyme; P-XYGLN, >95 %), and 1 % xylan (Xyl) from birchwood (Megazyme; P-ACXYL). The reaction mixtures containing Avicel® were incubated for 3.5 h in shaking. Boiled enzyme samples and supernatants from cultures with the empty vector were used as negative controls. The absorbance values were translated into amounts of reducing sugars released using a standard curve generated from glucose.

2.9. Statistical analysis

All data were reported as the means ± SEs of at least three biological replicates. Significant differences in gene expression between fruit ripening stages were assessed using ANOVA, followed by Tukey's post-hoc test ($P < 0.05$) on $\log_2$ transformed data. Significant differences in gene expression after ABA treatment were assessed using Student's *t*-test ($P \leq 0.05$) on $\log_2$ transformed data.

3. Results and discussion

3.1. Physicochemical characteristics of bilberry cellulases

Based on sequence similarity and conserved domain analyses, 20 full-length GH9 cellulases were identified in this study from the bilberry genome. Among the 20 bilberry cellulase genes, four (20 %) encoded membrane-anchored A-types, 14 (70 %) encoded secreted B-types, and two (10 %) encoded secreted enzymes with a carbohydrate binding module 49 (CBM49) and were thus classified as C-types (Table 1). Both the number of GH9 members and their relative abundance in the three subgroups in the bilberry genome were similar to those reported for other plant species in previous studies (Buchanan et al., 2012).

In all bilberry cellulases, the GH9 catalytic domain was highly conserved, revealing a large cellulose-degrading potential. However, the cellulases showed wide variations in size, with A-types ranging from 424 to 626 amino acids (AA), B-types from 474 to 532 AA and C-types from 593 to 629 AA in length (Table 1). The protein sequences also showed wide variations in predicted isoelectric points (p*I*) ranging from 4.94 to 8.93. Given the highly conserved GH9 catalytic domain, much of the variation in the physicochemical properties can thus be attributed to sequences flanking the GH9 catalytic domain at the N-terminus, such as the transmembrane domain (TMD) and signal peptide (SP) and C-terminal CBM49. The bilberry cellulases were named according to the nomenclature proposed for plant cellulases by Urbanowicz, Bennett, et al. (2007). The relative abundance of the different subtypes and their diverse physicochemical properties suggest that the bilberry cellulase arsenal is capable of depolymerizing cellulose under potentially wide physiological conditions in the plant.

3.2. Phylogeny analysis indicates B- and C-type cellulases in fruit softening

Phylogenetic analysis was performed on full-length bilberry cellulases and GH9 sequences from other plant species (**Supplementary Table S1**). The phylogenetic tree revealed seven major clusters, indicating similarities in domain structures as well as in sequences supported by high bootstrap values (>70 %) (Fig. 1). The four membrane-anchored A-type bilberry cellulases formed a discrete cluster with functionally characterized A-type cellulases reported previously from *A. thaliana* (Mølhøj et al., 2002). Conversely, the secreted bilberry proteins formed several clusters with orthologs from other plants, further highlighting the potential diversity of the physiological processes in which cellulases play a role. The phylogenetic tree revealed that some of the bilberry cellulases clustered closely with B- and C-type cellulases that have been associated with fruit softening in previous studies. Particularly, VmGH9B6 was grouped in the same clade as the fruit ripening-specific cellulases FaEG1 (FraCel1) from strawberry and SlCel2 from tomato (Fig. 1), which have previously been shown to affect fruit firmness by antisense and knockout studies, respectively (Jara et al., 2019; Lashbrook et al., 1994; Lee & Kim, 2011; Su et al., 2024). Conversely, C-type cellulases formed their own clade, where VmGH9C1 and VmGH9C2 clustered with mango MiCel1 and strawberry FaCel2 (FaEG3), both of which have been reported to have fruit ripening-specific gene expression (Chourasia et al., 2008; Llop-Tous et al., 1999). This clustering pattern indicates the involvement of bilberry B- and C-type cellulases in fruit softening.

3.3. Four bilberry cellulases show fruit ripening-specific expression

The expression levels of bilberry cellulase genes were investigated using the transcriptome data generated from ripening bilberry fruit in our previous study (Samkumar et al., 2021). Four secreted B/C-type cellulase genes, namely *VmGH9B4, VmGH9B6, VmGH9C1,* and *VmGH9C2*, showed high transcript levels in the berries (**Supplementary Table S4**). A closer analysis of the expression levels in bilberry tissues by

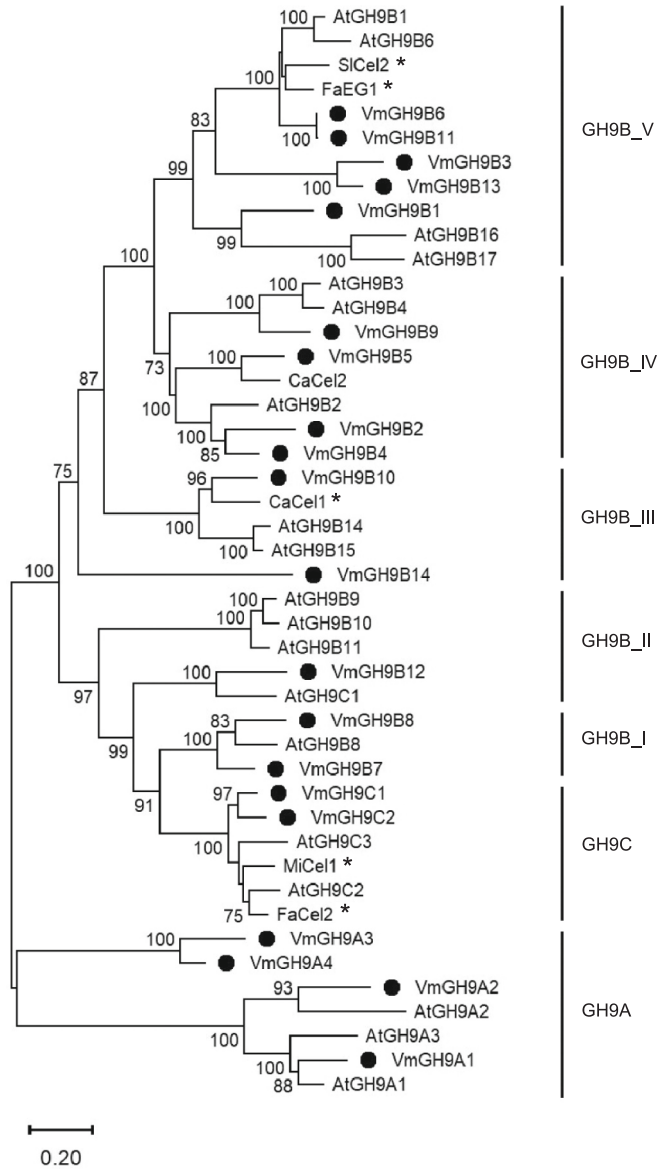

Fig. 1. Phylogenetic tree of bilberry cellulases and homologs from other plant species. The tree was constructed using the Maximum Likelihood method with 1000 bootstrap replications in MEGA 11. Each number represents the bootstrap value for each node (only values >60 % are shown). The black circles show cellulases from bilberry. Asterisks (*) represent cellulases that have been previously indicated in fruit ripening and softening. The first two letters in the protein names represent the plant species as follows: At, *Arabidopsis thaliana*; Ca, *Capsicum annuum;* Fa, *Fragaria* × *ananassa*; Mi, *Mangifera indica*; Sl, *Solanum lycopersicum* and Vm, *Vaccinium myrtillus*.

RT-qPCR confirmed that their expression was the highest in berries (Fig. 2A; **Supplementary Fig. S1A**) and during fruit ripening (stages 3.5–5.0), with slightly different, however, overlapping expression patterns (Fig. 2B; **Supplementary Fig. S1B**). The expression levels of *VmGH9B4* and *VmGH9C1* peaked earlier (stage 3.5) than those of *VmGH9B6* and *VmGH9C2* (stage 4.5). Our results indicate that *VmGH9B4, VmGH9B6, VmGH9C1,* and *VmGH9C2* are the best candidate genes to be involved in the processes associated with fruit ripening and softening in bilberries. Our suggestion is supported by the results of previous studies in mango and strawberry, where the accumulation of cellulase gene transcripts during fruit ripening was accompanied by a loss of fruit firmness and reduced cellulose/hemicellulose content (Chourasia et al., 2008; Jara et al., 2019).

Furthermore, the expression of these four bilberry cellulases was significantly induced by the ABA treatment in unripe bilberries (Fig. 2C; **Supplementary Fig. S1C**). ABA is known as a key plant hormone that regulates fruit ripening in bilberry and other fruits and plays a role in controlling the expression of a range of fruit softening genes (Karppinen et al., 2018; Mattus-Araya et al., 2023; Sun et al., 2012). Notably, *VmGH9B4* expression decreased at higher ABA concentration (2 mM) and peaked at the early fruit ripening stage 3.5, which may indicate sensitivity to ABA or other compounds that accumulate in ripening berries, such as sugars. Based on our previous studies, various sugars, including glucose, fructose, and sucrose are known to accumulate during bilberry fruit ripening (Samkumar et al., 2022). In some previous biochemical studies, high concentrations of sugars have been reported to inhibit cellulase activity in *in vitro* assays (Ferchak & Pye, 1983; Hsieh et al., 2014). Whether such regulation of cellulases in bilberry exists, remains to be investigated in further studies.

3.4. *Bilberry cellulases exhibit industrially relevant biochemical properties*

Following the identification of *VmGH9B4, VmGH9B6, VmGH9C1,* and *VmGH9C2* as the cellulase genes potentially playing crucial roles in cell wall depolymerization in bilberry fruit, we cloned the genes into the pPICZαA expression plasmid and produced them as recombinant proteins in *Pichia pastoris* for analyses of their enzymatic properties. In Western blot analysis, protein bands corresponding to the expected molecular weights of the recombinant cellulases were observed, as well as either lower or higher molecular weight bands in some instances (Fig. 3A). The lower molecular weight bands could be attributed to protein degradation, whereas the higher molecular weight bands could be the result of either extensive post-translational modifications of the recombinant proteins or recombinant protein aggregation. Recombinant proteins produced in *P. pastoris* heterologous systems have been reported to undergo N- or O-glycosylation of asparagine and serine or threonine, respectively, where sugar residues are covalently linked to the protein, thereby increasing their molecular weight (Bretthauer & Castellino, 1999).

When cellulase assays were performed for the recombinant enzymes using the carboxymethylcellulose (CMC) as a substrate, VmGH9C1 exhibited maximum activity at pH 6 and maintained a relatively high activity (>94 %) over pH 7–10 (Fig. 3B), showing that it is relatively insensitive to alkaline pH. This pH optimum is similar to that reported previously for recombinant cellulases of plant origin (Liebminger et al., 2013; Mølhøj et al., 2001). On the other hand, VmGH9B4 and VmGH9C2 and VmGH9B6 showed the highest activity at alkaline pH 8 and 9, respectively, but were generally more sensitive to further increases in pH than VmGH9C1 (Fig. 3B). These alkaline pH optima for bilberry cellulases are different from those of recombinant cellulases described from plants (Liebminger et al., 2013; Mølhøj et al., 2001), though more similar to those of cellulases characterized earlier from bacteria (Hmad & Gargouri, 2017; Horikoshi et al., 1984). Overall, all the recombinant bilberry cellulase enzymes maintained relatively high activity at pH ranging from 6 to 10. Another notable property of bilberry cellulases was that they retained their activity over a wide range of temperatures. All the tested recombinant bilberry cellulases showed optimal activity at 70 °C, which dropped rapidly to <3 % at 80 °C (Fig. 3C). This high temperature optimum is not typical for plant cellulases, however, is more similar to cellulases reported previously in some bacterial and fungal cellulases, mainly from thermophilic environments (Liang et al., 2011; Tucker et al., 1989).

Thermal stability analysis further revealed differences in the thermotolerance of the recombinant bilberry cellulases. All the enzymes showed a decrease in residual activity after 30 min of incubation at all temperatures, except for VmGH9B6 at 50 °C (Fig. 4). VmGH9C1 was thermally more stable between 30 and 70 °C and retained a higher activity (at least 63.6 %) after a 120 min incubation period compared to VmGH9C2 (45.5 %), VmGH9B4 (47.9 %), and VmGH9B6 (41.1 %).

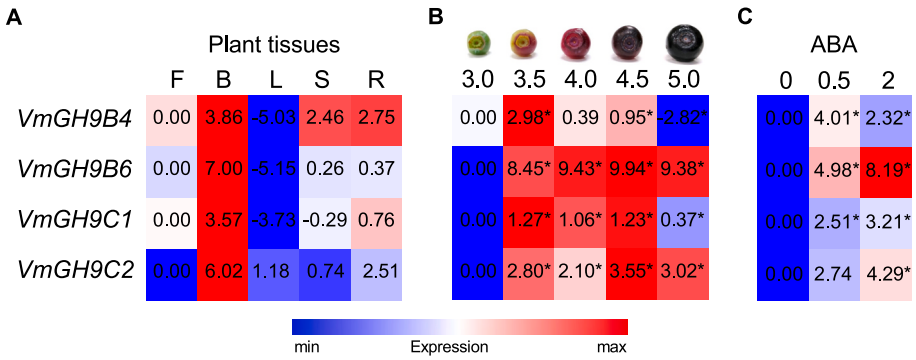

Fig. 2. Expression profiles of *VmGH9* genes in bilberry. (A) Expression of *VmGH9* genes in bilberry tissues. F, flower; B, ripening berry; L, leaf; S, stem; R, rhizome. (B) Expression of *VmGH9* genes during bilberry fruit ripening from stage 3.0 (unripe green) to stage 5.0 (fully ripe blue). Asterisks (*) indicate significant differences compared to stage 3.0 assessed using ANOVA followed by Tukey's post-hoc test ($P \leq 0.05$) on $\log_2$ transformed data. (C) Expression of *VmGH9* genes in abscisic acid (ABA)-treated bilberry fruits quantified after 48 h from the beginning of the treatment (0.5 mM ABA, 2 mM ABA or water as negative control). Asterisks (*) indicate significant differences compared to control assessed by Student's *t*-test ($P \leq 0.05$) on $\log_2$ transformed data. All values represent means of at least three replicates. Red and blue boxes indicate high and low relative expression levels, respectively.

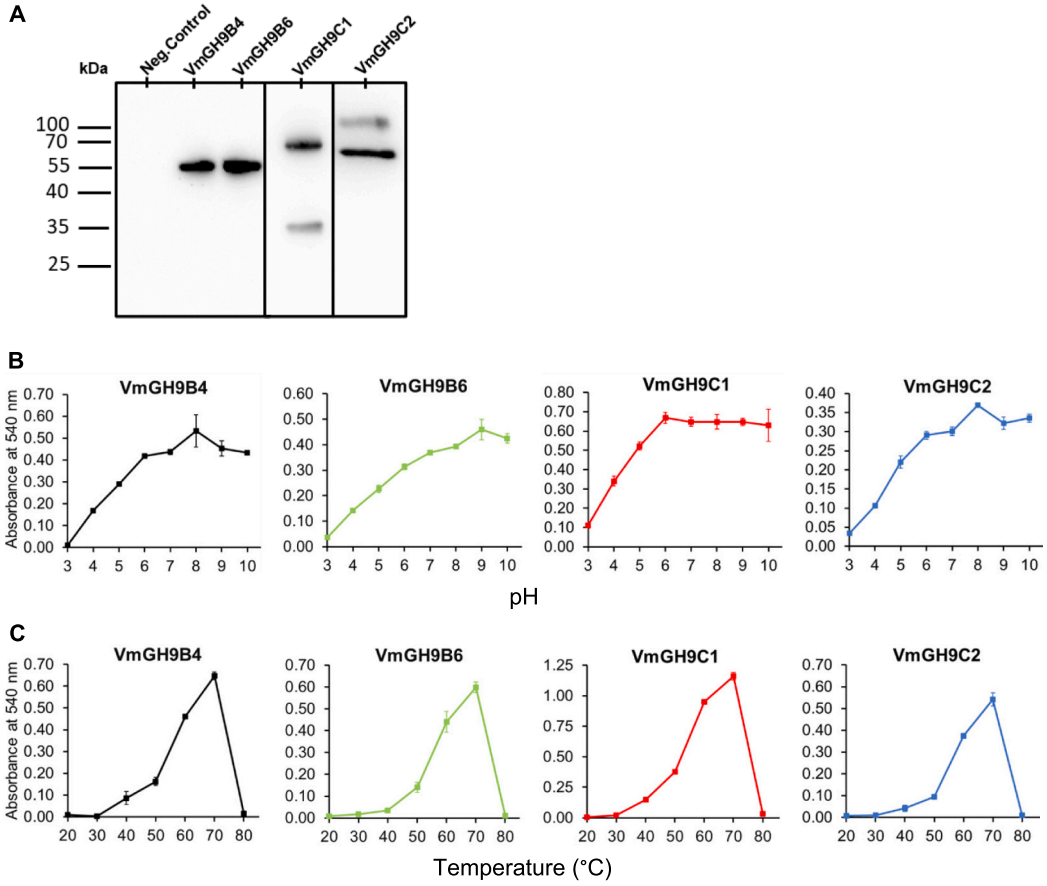

Fig. 3. Biochemical properties of recombinant bilberry cellulases. (A) Analysis of GH9 recombinant protein secretion by *Pichia pastoris* using Western blot. The numbers on the left represent molecular weights of the protein ladder in kilodaltons (kDa). Neg.Control represents the empty vector control. Expected molecular weights of the recombinant proteins: VmGH9B4, 55.55 kDa; VmGH9B6, 53.72 kDa; VmGH9C1, 67.24 kDa and VmGH9C2, 64.05 kDa. (B) Optimal pH and (C) temperature for recombinant bilberry cellulase enzymes. Enzyme activity was measured by the DNS method using CMC as substrate, and level of activities are shown as absorbance at 540 nm. Data represent means ± SEs of three replicates.

Similar results have been reported earlier for cellulases from bacteria and fungi that showed thermal stability from 30 to 70 °C (Deka et al., 2013; Jin et al., 2020; Pandey et al., 2014). Interestingly, the residual activity of VmGH9B6 at 50 °C increased gradually over time and was >100 % after 120 min incubation. None of the cellulases were completely inactivated even after incubation at 80 °C for 120 min, retaining at least 30.1 % of the initial activity (Fig. 4), which could be attributed to the stabilizing effect of glycerol, which concurs with some observations in earlier studies (Wang et al., 2022). The optimal temperature of 70 °C for the recombinant bilberry cellulases was higher than that reported for endoglucanase I from the industrially important fungus, *Trichoderma reesei* (Chokhawala et al., 2015). Compared to *T. reesei*,

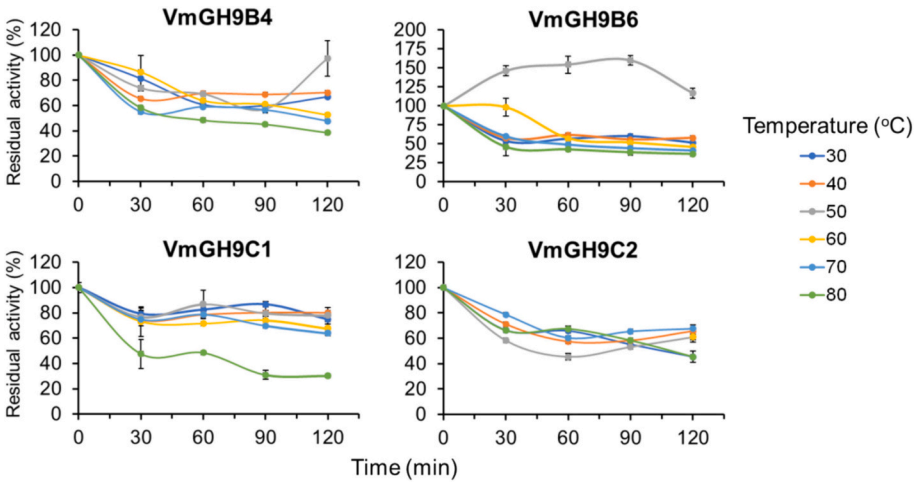

Fig. 4. Thermal stability of recombinant bilberry cellulases. Recombinant enzymes were produced in *Pichia pastoris* as a host. Thermal stability was determined by incubating each enzyme at temperatures ranging from 30 to 80 °C for 30, 60, 90, and 120 min. Residual enzyme activity was measured using the DNS method with CMC as substrate and expressed as a percentage of the maximum enzyme activity under optimal assay conditions. Data represent means ± SEs of three replicates.

bilberry cellulases further showed superior thermal stability between 50 and 70 °C and this thermal property is only similar to those reported for thermophilic fungi, including *Chaetomium thermophilum*, *Thermoascus aurantiacus,* and *Acremonium thermophilum* (Viikari et al., 2007). Thus, the bilberry cellulases analyzed in this study appear to possess a mix of microbial cellulase-like biochemical properties, which contradicts the fact that this plant is geographically confined to cold places. However, these properties are highly plausible and may be relics from their ancestral bacterial relatives, as shown by Kundu and Sharma (2018). High temperature optima and enzyme stability at high temperatures would permit biomass degradation at elevated temperatures with the associated benefits of high specific activity, reduced growth of contaminating microbes, and higher biomass loading due to reduced viscosity at elevated temperatures. As high temperature optima and thermal stability have become important properties for the industrial application of enzymes, the bilberry cellulases possess a great potential for applications in industrial bioprocessing, especially in cellulose degradation.

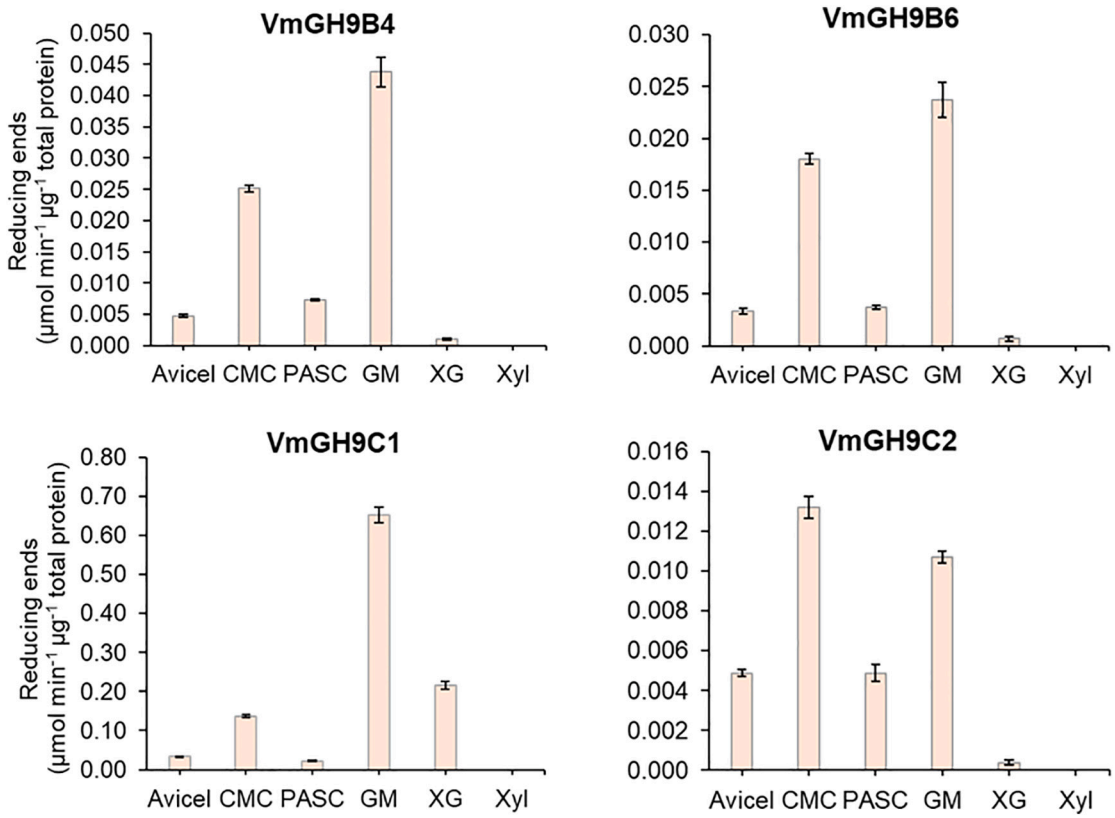

Fig. 5. Activity of recombinant bilberry cellulases on cellulosic and hemicellulosic substrates. Recombinant enzymes were produced in a *Pichia pastoris* heterologous system. Enzyme activity was measured by the DNS method and reaction mixtures were incubated at optimal pH and temperature for each enzyme. Enzyme activities are presented as the amount of reducing ends in micromoles released per minute per microgram of total protein. Bars represent means ± SEs of three replicates. CMC, carboxymethylcellulose; PASC, phosphoric acid swollen cellulose; GM, glucomannan; XG, xyloglucan; Xyl, xylan.

3.5. Bilberry cellulases degrade both cellulose and hemicelluloses

To assess the potential of the bilberry recombinant cellulases, hydrolytic enzyme activities were evaluated against relevant cellulosic and hemicellulosic substrates. All the enzymes showed ability to degrade CMC, microcrystalline cellulose Avicel®, phosphoric acid swollen cellulose (PASC), glucomannan (GM), xyloglucan (XG), but not xylan (Xyl) (Fig. 5). Among the cellulosic substrates, all the enzymes showed preference for soluble cellulose CMC followed by insoluble PASC and Avicel®. This is not surprising considering that CMC contains more readily accessible β-(1,4)-glucoside bonds compared to Avicel® which consists of highly packed and organized cellulose chains, leading to a lower amount of accessible surface area (Park et al., 2010; Pellegrini et al., 2018).

Concerning hemicellulose substrates, all the bilberry recombinant enzymes were able to degrade hemicelluloses (Fig. 5). While the hydrolytic activities of plant GH9 cellulases toward XG are generally described in the literature to be low (Urbanowicz, Catalá, et al., 2007), VmGH9C1 could efficiently degrade XG. Furthermore, all the bilberry recombinant cellulases could degrade GM with surprisingly high efficiency, and the hydrolytic activities of VmGH9B4, VmGH9B6, and VmGH9C1 were higher on GM than in any of the cellulosic substrates. Preference toward GM has been reported previously to be uncharacteristic for endoglucanases (Master et al., 2004; Yoshida & Komae, 2006), which mainly cleave the β-(1 → 4)-glycosidic linkages. However, konjac GM, that was used in this study, is known to contain about 40 % of β-(1 → 4)-linkages to glucose and 60 % to mannans, and also branches via β-(1 → 6)-linkages to glucose with degree of branching estimated to be at 8 % (Katsuraya et al., 2003). The presence of contiguous stretches of β-(1 → 4)-glucosidic linkages render GM a likely substrate for cellulases, however, the extent of depolymerization observed here, measured as the amount reducing ends released, can only be accounted for by an extensive depolymerization, possibly including the cleavage of linkages between mannose residues. Earlier, some plant GH9 enzymes have been suggested to degrade XG and GM in fruits (Dheilly et al., 2016; Jara et al., 2019; Su et al., 2024). In dicot primary cell walls, including those of fruits, hemicelluloses are known to consist mainly of XG, GM, and Xyl (Assor et al., 2013; Vicante et al., 2007) and XG degradation is generally considered to be high (Moya-León et al., 2019; Olmedo et al., 2021). Previously, Dheilly et al. (2016) connected GH9 activity to GM degradation in the early ripening stage of apple fruit, which is consistent with our observations of *VmGH9B4* and *VmGH9C1* expression during the early fruit ripening and the high preference of the recombinant enzymes for GM.

We further revealed that VmGH9C1 showed remarkably high activity compared to the other bilberry enzymes evaluated in this study, reaching 0.65 μmol min^{-1} $μg^{-1}$ on GM (Fig. 5). In terms of activity on cellulosic substrates, VmGH9C1 showed at least 6-, 5- and 3-fold higher activity on Avicel®, CMC and PASC, respectively, compared to other bilberry recombinant cellulases (Table 2). Among the hemicellulosic substrates, VmGH9C1 activity on GM and XG was at least 14- and 215-fold higher, respectively, compared to other bilberry cellulases (Table 2). Thus, VmGH9C1 could be considered as a specific candidate for further optimization for actual bioprocessing applications.

Table 2
Ratio of relative activities of recombinant bilberry cellulases on different substrates.[a]

Substrate	C1:B4	C1:B6	C1:C2	B4:B6	B4:C2	B6:C2
Avicel®	6.87	9.74	6.73	1.42	0.98	0.69
CMC	5.43	7.58	10.36	1.39	1.91	1.37
PASC	3.01	5.87	4.52	1.95	1.50	0.77
GM	14.90	27.51	61.01	1.85	4.09	2.22
XG	215.79	314.38	549.33	1.46	2.55	1.75
Xyl	0.00	0.00	0.00	0.00	0.00	0.00

[a] Relative activity was calculated as the ratio of the activity of one enzyme on a given substrate to activity of the other enzyme on the same substrate. C1, VmGH9C1; C2, VmGH9C2; B4, VmGH9B4 and B6, VmGH9B6.

4. Conclusions

Four GH9 cellulases have been identified in bilberry that are likely to be involved in cell wall depolymerization during fruit softening. The recombinant cellulase enzymes showed hydrolytic activity toward recalcitrant cellulose, XG and GM, which are the most abundant polysaccharides in plant biomass. In particular, VmGH9C1 demonstrated superior activity against all substrates compared to the other cellulases tested. The hydrolytic properties of VmGH9C1 combined with a wide pH and temperature range as well as thermal stability between 30 and 70 °C are desirable attributes for industrial bioprocessing applications. This versatile enzyme could be subjected to further investigation and optimization of its performance, for example, by testing synergy with expansin proteins, as well as testing its production in various heterologous systems and extraction from berry industry side-streams.

Funding

This work was supported by local funds from the Arctic Centre for Sustainable Energy (ARC) at UiT in years 2020 and 2022 (to KK).

CRediT authorship contribution statement

Hilary Edema: Data curation, Formal analysis, Investigation, Methodology, Visualization, Writing – original draft. Muhammad Furqan Ashraf: Investigation, Validation. Amos Samkumar: Data curation, Investigation, Writing – review & editing. Laura Jaakola: Conceptualization, Resources, Supervision, Writing – review & editing. Katja Karppinen: Conceptualization, Formal analysis, Investigation, Funding acquisition, Project administration, Resources, Supervision, Visualization, Writing – review & editing. All authors read and approved the final manuscript.

Declaration of competing interest

The authors declare that they have no known competing financial interests or personal relationships that could have appeared to influence the work reported in this paper.

Data availability

No data was used for the research described in the article.

Acknowledgements

The authors are grateful to Dr. Tanja Paasela and Dr. Wiebke Haeger for providing with the *P. pastoris* strains and expression plasmids used in this study. We thank MSc. Fjodor van Steenis for help with qPCR analysis of GH9 gene expression in ripening fruits. We are grateful to Alena Didriksen, Manon Seyer, and Marc Rams i Ríos for supporting the analysis of the optimal temperature and pH for recombinant cellulases.

Appendix A. Supplementary data

Supplementary data to this article can be found online at https://doi.org/10.1016/j.carbpol.2024.122493.

References

Almagro Armenteros, J. J., Tsirigos, K. D., Sønderby, C. K., Petersen, T. N., Winther, O., Brunak, S., … Nielsen, H. (2019). SignalP 5.0 improves signal peptide predictions using deep neural networks. *Nature Biotechnology, 37*, 420–423.

Anders, S., Pyl, P. T., & Huber, W. (2015). HTSeq–a Python framework to work with high-throughput sequencing data. *Bioinformatics, 31*, 166–169.

Assor, C., Quemener, B., Vigouroux, J., & Lahaye, M. (2013). Fractionation and structural characterization of LiCl-DMSO soluble hemicelluloses from tomato. *Carbohydrate Polymers, 94*, 46–55.

Bretthauer, R. K., & Castellino, F. J. (1999). Glycosylation of *Pichia pastoris*-derived proteins. *Biotechnology and Applied Biochemistry, 30*, 193–200.

Buchanan, M., Burton, R. A., Dhugga, K. S., Rafalski, A. J., Tingey, S. V., Shirley, N. J., & Fincher, G. B. (2012). Endo-(1,4)-β-glucanase gene families in the grasses: temporal and spatial co-transcription of orthologous genes. *BMC Plant Biology, 12*, 235.

del Campillo, E. (1999). Multiple endo-1,4-β-D-glucanase (cellulase) genes in *Arabidopsis*. *Current Topics in Developmental Biology, 46*, 39–61.

Ceja-Navarro, J. A., Karaoz, U., Bill, M., Hao, Z., White, R. A., III, Arellano, A., … Brodie, E. L. (2019). Gut anatomical properties and microbial functional assembly promote lignocellulose deconstruction and colony subsistence of a wood-feeding beetle. *Nature Microbiology, 4*, 864–875.

Chokhawala, H. A., Roche, C. M., Kim, T. W., Atreya, M. E., Vegesna, N., Dana, C. M., … Clark, D. S. (2015). Mutagenesis of *Trichoderma reesei* endoglucanase I: impact of expression host on activity and stability at elevated temperatures. *BMC Biotechnology, 15*, 11.

Chourasia, A., Sane, V. A., Singh, R. K., & Nath, P. (2008). Isolation and characterization of the *MiCel1* gene from mango: ripening related expression and enhanced endoglucanase activity during softening. *Plant Growth Regulation, 56*, 117–127.

Costa, F. F., de Oliveira, D. T., Brito, Y. P., da Rocha Filho, G. N., Alvarado, C. G., Balu, A. M., … do Nascimento, L. A. S. (2020). Lignocellulosics to biofuels: An overview of recent and relevant advances. *Current Opinion in Green and Sustainable Chemistry, 24*, 21–25.

Cragg, S. M., Beckham, G. T., Bruce, N. C., Bugg, T. D. H., Distel, D. L., Dupree, P., … Zimmer, M. (2015). Lignocellulose degradation mechanisms across the tree of life. *Current Opinion in Chemical Biology, 29*, 108–119.

Deka, D., Jawed, M., & Goyal, A. (2013). Purification and characterization of an alkaline cellulase produced by *Bacillus subtilis* (AS3). *Preparative Biochemistry & Biotechnology, 43*, 256–270.

Dheilly, E., Le Gall, S., Guillou, M. C., Renou, J. P., Bonnin, E., Orsel, M., & Lahaye, M. (2016). Cell wall dynamics during apple development and storage involves hemicellulose modifications and related expressed genes. *BMC Plant Biology, 16*, 201.

Drula, E., Garron, M. L., Dogan, S., Lombard, V., Henrissat, B., & Terrapon, N. (2022). The carbohydrate-active enzyme database: functions and literature. *Nucleic Acids Research, 50*, D571–D577.

Du, Q., Wang, L., Yang, X., Gong, C., & Zhang, D. (2015). *Populus* endo-β-1,4-glucanases gene family: genomic organization, phylogenetic analysis, expression profiles and association mapping. *Planta, 241*, 1417–1434.

Duvaud, S., Gabella, C., Lisacek, F., Stockinger, H., Ioannidis, V., & Durinx, C. (2021). Expasy, the Swiss Bioinformatics Resource Portal, as designed by its users. *Nucleic Acids Research, 49*, W216–W227.

Ejaz, U., Sohail, M., & Ghanemi, A. (2021). Cellulases: From bioactivity to a variety of industrial applications. *Biomimetics, 6*, 44.

Elhassan, S. Y. M., & Abu-Goukh, A. B. A. (2016). Role of cellulase enzyme in fruit softening during muskmelon fruit ripening. *American Journal of Scientific and Industrial Research, 7*, 98–105.

Ferchak, J. D., & Pye, E. K. (1983). Effect of cellobiose, glucose, ethanol, and metal ions on the cellulase enzyme complex of *Thermomonospora fusca*. *Biotechnology and Bioengineering, 25*, 2865–2872.

Figueroa, C. R., Rosli, H. G., Civello, P. M., Martínez, G. A., Herrera, R., & Moya-León, M. A. (2010). Changes in cell wall polysaccharides and cell wall degrading enzymes during ripening of *Fragaria chiloensis* and *Fragaria* × *ananassa* fruits. *Scientia Horticulturae, 124*, 454–462.

Grandis, A., de Souza, A. P., Tavares, E. Q. P., & Buckeridge, M. S. (2014). Using natural plant cell wall degradation mechanisms to improve second generation bioethanol. In M. C. McCann, M. Buckeridge, & N. Carpita (Eds.), *Plants and bioenergy. Advances in plant biology 4* (pp. 211–230). New York: Springer.

Grandis, A., Leite, D. C. C., Tavares, E. Q. P., Arenque-Musa, B. C., Gaiarsa, J. W., Martins, M. C. M., … Buckeridge, M. S. (2019). Cell wall hydrolases act in concert during aerenchyma development in sugarcane roots. *Annals of Botany, 124*, 1067–1089.

Gupta, R., Mehta, G., Deswal, D., Sharma, S., Jain, K. K., Singh, A., & Kuhad, R. C. (2013). Cellulases and their biotechnological applications. In R. C. Kuhad, & A. Singh (Eds.), *Biotechnology for environmental management and resource recovery* (pp. 89–106). New Delhi: Springer.

He, H., Bai, M., Tong, P., Hu, Y., Yang, M., & Wu, H. (2018). CELLULASE6 and MANNANASE7 affect cell differentiation and silique dehiscence. *Plant Physiology, 176*, 2186–2201.

He, Z. J., Chen, K., Liu, Z. H., Li, B. Z., & Yuan, Y. J. (2023). Valorizing renewable cellulose from lignocellulosic biomass towards functional products. *Journal of Cleaner Production, 414*, Article 137708.

Hiller, K., Grote, A., Scheer, M., Münch, R., & Jahn, D. (2004). PrediSi: prediction of signal peptides and their cleavage positions. *Nucleic Acids Research, 32*, W375–W379.

Hmad, I. B., & Gargouri, A. (2017). Neutral and alkaline cellulases: Production, engineering, and applications. *Journal of Basic Microbiology, 57*, 653–658.

Horikoshi, K., Nakao, M., Kurono, Y., & Sashihara, N. (1984). Cellulases of an alkalophilic *Bacillus* strain isolated from soil. *Canadian Journal of Microbiology, 30*, 774–779.

Hsieh, C. W. C., Cannella, D., Jørgensen, H., Felby, C., & Thygesen, L. G. (2014). Cellulase inhibition by high concentrations of monosaccharides. *Journal of Agricultural and Food Chemistry, 62*, 3800–3805.

Jara, K., Castro, R. I., Ramos, P., Parra-Palma, C., Valenzuela-Riffo, F., & Morales-Quintana, L. (2019). Molecular insights into FaEG1, a strawberry endoglucanase enzyme expressed during strawberry fruit ripening. *Plants, 8*, 140.

Jin, X., Song, J., Ma, J., & Liu, G. Q. (2020). Thermostable β-xylosidase from *Aspergillus fumigatus*: Purification, characterization, and potential application in lignocellulose bioethanol production. *Renewable Energy, 155*, 1425–1431.

Karppinen, K., Tegelberg, P., Häggman, H., & Jaakola, L. (2018). Abscisic acid regulates anthocyanin biosynthesis and gene expression associated with cell wall modification in ripening bilberry (*Vaccinium myrtillus* L.) fruits. *Frontiers. Plant Science, 9*, 1259.

Katsuraya, K., Okuyama, K., Hatanaka, K., Oshima, R., Sato, T., & Matsuzaki, K. (2003). Constitution of konjac glucomannan: chemical analysis and ^{13}C NMR spectroscopy. *Carbohydrate Polymers, 53*, 183–189.

Kundu, S., & Sharma, R. (2018). Origin, evolution, and divergence of plant class C GH9 endoglucanases. *BMC Evolutionary Biology, 18*, 79.

Lashbrook, C. C., Gonzalez-Bosch, C., & Bennett, A. B. (1994). Two divergent endo-β-1,4-glucanase genes exhibit overlapping expression in ripening fruit and abscising flowers. *The Plant Cell, 6*, 1485–1493.

Lee, Y. K., & Kim, I. J. (2011). Modulation in fruit softening by antisense suppression of endo-β-1,4-glucanase in strawberry. *Molecular Breeding, 27*, 375–383.

Li, C., Wang, Y., Ying, P., Ma, W., & Li, J. (2015). Genome-wide digital transcript analysis of putative fruitlet abscission related genes regulated by ethephon in litchi. *Frontiers in Plant Science, 6*, 502.

Li, C., Zhao, M., Ma, X., Wen, Z., Ying, P., Peng, M., … Li, J. (2019). The HD-Zip transcription factor LcHB2 regulates litchi fruit abscission through the activation of two cellulase genes. *Journal of Experimental Botany, 70*, 5189–5203.

Li, T., Chen, C., Brozena, A. H., Zhu, J. Y., Xu, L., Driemeier, C., … Hu, L. (2021). Developing fibrillated cellulose as a sustainable technological material. *Nature, 590*, 47–56.

Liang, C., Fioroni, M., Rodríguez-Ropero, F., Xue, Y., Schwaneberg, U., & Ma, Y. (2011). Directed evolution of a thermophilic endoglucanase (Cel5A) into highly active Cel5A variants with an expanded temperature profile. *Journal of Biotechnology, 154*, 46–53.

Liebminger, E., Grass, J., Altmann, F., Mach, L., & Strasser, R. (2013). Characterizing the link between glycosylation state and enzymatic activity of the endo-β1,4-glucanase KORRIGAN1 from *Arabidopsis thaliana*. *The Journal of Biological Chemistry, 288*, 22270–22280.

Liu, J., Zhao, Y., Xu, H., Zhao, X., Tan, Y., Li, P., Li, D., Tao, Y., & Liu, D. (2021). Fruit softening correlates with enzymatic activities and compositional changes in fruit cell wall during growing in *Lycium barbarum* L. *International Journal of Food Science and Technology, 56*, 3044–3054.

Llop-Tous, I., Domínguez-Puigjaner, E., Palomer, X., & Vendrell, M. (1999). Characterization of two divergent endo-β-1,4-glucanase cDNA clones highly expressed in the nonclimacteric strawberry fruit. *Plant Physiology, 119*, 1415–1421.

Lopez-Casado, G., Urbanowicz, B. R., Damasceno, C. M. B., & Rose, J. K. C. (2008). Plant glycosyl hydrolases and biofuels: a natural marriage. *Current Opinion in Plant Biology, 11*, 329–337.

Madeira, F., Pearce, M., Tivey, A. R. N., Basutkar, P., Lee, J., Edbali, O., … Lopez, R. (2022). Search and sequence analysis tools services from EMBL-EBI in 2022. *Nucleic Acids Research, 50*, W276–W279.

Maitan-Alfenas, G. P., Visser, E. M., & Guimarães, V. M. (2015). Enzymatic hydrolysis of lignocellulosic biomass: converting food waste in valuable products. *Current Opinion in Food Science, 1*, 44–49.

Master, E. R., Rudsander, U. J., Zhou, W., Henriksson, H., Divne, C., Denman, S., … Teeri, T. T. (2004). Recombinant expression and enzymatic characterization of PttCel9A, a KOR homologue from *Populus tremula* × *tremuloides*. *Biochemistry, 43*, 10080–10089.

Mattus-Araya, E., Stappung, Y., Herrera, R., & Moya-León, M. A. (2023). Molecular actors involved in the softening of *Fragaria chiloensis* fruit accelerated by ABA treatment. *Journal of Plant Growth Regulation, 42*, 433–448.

Mejía-Mendoza, M. A., Garcidueñas-Piña, C., Padilla-Ramírez, J. S., Soria-Guerra, R. E., & Morales-Domínguez, J. F. (2022). Identification in silico and expression analysis of a β-1-4-endoglucanase and β-galactosidase genes related to ripening in guava fruit. *Journal of Genetic Engineering and Biotechnology, 20*, 3.

Menon, V., & Rao, M. (2012). Trends in bioconversion of lignocellulose: Biofuels, platform chemicals & biorefinery concept. *Progress in Energy and Combustion Science, 38*, 522–550.

Miller, G. L. (1959). Use of dinitrosalicylic acid reagent for determination of reducing sugar. *Analytical Chemistry, 31*, 426–428.

Ming, R., Hou, S., Feng, Y., Yu, Q., Dionne-Laporte, A., Saw, J. H., … Alam, M. (2008). The draft genome of the transgenic tropical fruit tree papaya (*Carica papaya* Linnaeus). *Nature, 452*, 991–996.

Mølhøj, M., Pagant, S., & Höfte, H. (2002). Towards understanding the role of membrane-bound endo-β-1,4-glucanases in cellulose biosynthesis. *Plant and Cell Physiology, 43*, 1399–1406.

Mølhøj, M., Ulvskov, P., & Dal Degan, F. (2001). Characterization of a functional soluble form of a *Brassica napus* membrane-anchored endo-1,4-β-glucanase heterologously expressed in *Pichia pastoris*. *Plant Physiology, 127*, 674–684.

Moya-León, M. A., Mattus-Araya, E., & Herrera, R. (2019). Molecular events occurring during softening of strawberry fruit. *Frontiers in Plant Science, 10*, 615.

Olmedo, P., Zepeda, B., Rojas, B., Silva-Sanzana, C., Delgado-Rioseco, J., Fernández, K., … Campos-Vargas, R. (2021). Cell wall calcium and hemicellulose have a role in the fruit firmness during storage of blueberry (*Vaccinium* spp.). *Plants, 10*, 553.

Pandey, S., Kushwah, J., Tiwari, R., Kumar, R., Somvanshi, V. S., Nain, L., & Saxena, A. K. (2014). Cloning and expression of β-1,4-endoglucanase gene from *Bacillus subtilis* isolated from soil long term irrigated with effluents of paper and pulp mill. *Microbiological Research, 169*, 693–698.

Park, S., Baker, J. O., Himmel, M. E., Parilla, P. A., & Johnson, D. K. (2010). Cellulose crystallinity index: measurement techniques and their impact on interpreting cellulase performance. *Biotechnology for Biofuels, 3*, 10.

Pellegrini, V. O. A., Bernardes, A., Rezende, C. A., & Polikarpov, I. (2018). Cellulose fiber size defines efficiency of enzymatic hydrolysis and impacts degree of synergy between endo- and exoglucanases. *Cellulose, 25*, 1865–1881.

Peng, Z., Liu, G., Li, H., Wang, Y., Gao, H., Jemrić, T., & Fu, D. (2022). Molecular and genetic events determining the softening of fleshy fruits: A comprehensive review. *International Journal of Molecular Sciences, 23*, 12482.

Potter, S. C., Luciani, A., Eddy, S. R., Park, Y., Lopez, R., & Finn, R. D. (2018). HMMER web server: 2018 update. *Nucleic Acids Research, 46*, W200–W204.

Real, M. D., Company, P., García-Agustín, P., Bennett, A. B., & González-Bosch, C. (2004). Characterization of tomato endo-β-1,4-glucanase Cel1 protein in fruit during ripening and after fungal infection. *Planta, 220*, 80–86.

Samkumar, A., Jones, D., Karppinen, K., Dare, A. P., Sipari, N., Espley, R. V., … Jaakola, L. (2021). Red and blue light treatments of ripening bilberry fruits reveal differences in signalling through abscisic acid-regulated anthocyanin biosynthesis. *Plant, Cell & Environment, 44*, 3227–3245.

Samkumar, A., Karppinen, K., Dhakal, B., Martinussen, I., & Jaakola, L. (2022). Insights into sugar metabolism during bilberry (*Vaccinium myrtillus* L.) fruit development. *Physiologia Plantarum, 174*, Article e13657.

Seddiqi, H., Oliaei, E., Honarkar, H., Jin, J., Geonzon, L. C., Bacabac, R. G., & Klein-Nulend, J. (2021). Cellulose and its derivatives: towards biomedical applications. *Cellulose, 28*, 1893–1931.

Shi, Y., Li, B. J., Grierson, D., & Chen, K. S. (2023). Insights into cell wall changes during fruit softening from transgenic and naturally occuring mutants. *Plant Physiology, 192*, 1671–1683.

Su, G., Lin, Y., Wang, C., Lu, J., Liu, Z., He, Z., … Chen, K. (2024). Expansin SlExp1 and endoglucanase SlCel2 synergistically promote fruit softening and cell wall disassembly in tomato. *The Plant Cell, 36*, 709–726.

Sun, L., Sun, Y., Zhang, M., Wang, L., Ren, J., Cui, M., … Leng, P. (2012). Suppression of 9-cis-epoxycarotenoid dioxygenase, which encodes a key enzyme in abscisic acid biosynthesis, alters fruit texture in transgenic tomato. *Plant Physiology, 158*, 283–298.

Tamura, K., Stecher, G., & Kumar, S. (2021). MEGA11: Molecular evolutionary genetics analysis version 11. *Molecular Biology and Evolution, 38*, 3022–3027.

Tavares, E. Q. P., de Souza, A. P., & Buckeridge, M. S. (2015). How endogenous plant cell-wall degradation mechanisms can help achieve higher efficiency in saccharification of biomass. *Journal of Experimental Botany, 66*, 4133–4143.

Tucker, M. P., Mohagheghi, A., Grohmann, K., & Himmel, M. E. (1989). Ultra-thermostable cellulases from *Acidothermus cellulolyticus*: Comparison of temperature optima with previously reported cellulases. *Biotechnology, 7*, 817–820.

Untergasser, A., Cutcutache, I., Koressaar, T., Ye, J., Faircloth, B. C., Remm, M., & Rozen, S. G. (2012). Primer3–new capabilities and interfaces. *Nucleic Acids Research, 40*, Article e115.

Urbanowicz, B. R., Bennett, A. B., del Campillo, E., Catalá, C., Hayashi, T., Henrissat, B., … Rose, J. K. C. (2007). Structural organization and a standardized nomenclature for plant endo-1,4-β-glucanases (cellulases) of glycosyl hydrolase family 9. *Plant Physiology, 144*, 1693–1696.

Urbanowicz, B. R., Catalá, C., Irwin, D., Wilson, D. B., Ripoll, D. R., & Rose, J. K. C. (2007). A tomato endo-β-1,4-glucanase, SlCel9C1, represents a distinct subclass with a new family of carbohydrate binding modules (CBM49). *The Journal of Biological Chemistry, 282*, 12066–12074.

Vasić, K., Knez, Ž., & Leitgeb, M. (2021). Bioethanol production by enzymatic hydrolysis from different lignocellulosic sources. *Molecules, 26*, 753.

Vicante, A. R., Ortugno, C., Rosli, H., Powell, A. L. T., Greve, L. C., & Labavitch, J. M. (2007). Temporal sequence of cell wall disassembly events in developing fruits. 2. Analysis of blueberry (*Vaccinium* species). *Journal of Agricultural and Food Chemistry, 55*, 4125–4130.

Victorica, M. R., Soria, M. A., Batista-García, R. A., Ceja-Navarro, J. A., Vikram, S., Ortiz, M., … Talia, P. M. (2020). Neotropical termite microbiomes as sources of novel plant cell wall degrading enzymes. *Scientific Reports, 10*, 3864.

Viikari, L., Alapuranen, M., Puranen, T., Vehmaanperä, J., & Siika-aho, M. (2007). Thermostable enzymes in lignocellulose hydrolysis. *Advances in Biochemical Engineering/Biotechnology, 108*, 121–145.

Wang, J., Chitsaz, F., Derbyshire, M. K., Gonzales, N. R., Gwadz, M., Lu, S., … Marchler-Bauer, A. (2023). The conserved domain database in 2023. *Nucleic Acids Research, 51*, D384–D388.

Wang, M., Sheng, Y., Cui, H., Li, A., Li, X., & Huang, H. (2022). The role of glycerol in preserving proteins needs to be reconsidered. *ACS Sustainable Chemistry & Engineering, 10*, 15175–15185.

Willis, J. D., Mazarei, M., & Stewart Jr, C. N. (2016). Transgenic plant-produced hydrolytic enzymes and the potential of insect gut-derived hydrolases for biofuels. *Frontiers in Plant Science, 7*, 675.

Wu, C., Deng, C., Hilario, E., Albert, N. W., Lafferty, D., Grierson, E. R. P., … Chagné, D. (2022). A chromosome-scale assembly of the bilberry genome identifies a complex locus controlling berry anthocyanin composition. *Molecular Ecology Resources, 22*, 345–360.

Yoshida, K., & Komae, K. (2006). A rice family 9 glycoside hydrolase isozyme with broad substrate specificity for hemicelluloses in type II cell walls. *Plant and Cell Physiology, 47*, 1541–1554.

Zhang, C., Xiong, Z., Lyu, L., Li, W., & Wu, W. (2023). Overexpression of blackberry *RuEG6* reduces the leaf cellulose content in tobacco. *Brazilian Journal of Botany, 46*, 27–33.

Zhang, C., Xiong, Z., Yang, H., & Wu, W. (2019). Changes in pericarp morphology, physiology and cell wall composition account for flesh firmness during the ripening of blackberry (*Rubus* spp.). *Scientia Horticulturae, 250*, 59–68.

Zhang, Y. H. P., Cui, J., Lynd, L. R., & Kuang, L. R. (2006). A transition from cellulose swelling to cellulose dissolution by *o*-phosphoric acid: Evidence from enzymatic hydrolysis and supramolecular structure. *Biomacromolecules, 7*, 644–648.

Zhu, Y., Guo, J., Wu, F., Yu, H., Min, J., Zhao, Y., & Xu, C. (2023). Genome-wide characteristics of GH9B family members in melon and their expression profiles under exogenous hormone and far-red light treatment during the grafting healing process. *International Journal of Molecular Sciences, 24*, 8258.

Zoghlami, A., & Paës, G. (2019). Lignocellulosic biomass: Understanding recalcitrance and predicting hydrolysis. *Frontiers in Chemistry, 7*, 874.

Zugenmaier, P. (2021). Order in cellulosics: Historical review of crystal structure research on cellulose. *Carbohydrate Polymers, 254*, Article 117417.